ANL-7303
Reactor Technology
(TID-4500)
AEC Research and
Development Report

ARGONNE NATIONAL LABORATORY
9700 South Cass Avenue
Argonne, Illinois 60439

THE EFFECTIVENESS OF CONTROL-ROD MATERIALS

by

H. P. Iskenderian

Reactor Physics Division

April 1967

TABLE OF CONTENTS

LIST OF FIGURES

LIST OF TABLES

THE EFFECTIVENESS OF CONTROL-ROD MATERIALS

by

H. P. Iskenderian

I. INTRODUCTION

Considerable work has been done on the evaluation of the worth of control-rod materials. Some of this is listed in Refs. 1-5.

References 1 and 2 describe a method of determining the "effectiveness" of control-rod materials, with experimental checks from the ZPR-1 critical assembly. The method consisted of the evaluation of the absorption integral for neutrons incident on a slab obeying the Breit-Wigner, single-level absorption characteristics. This report is an extension of Refs. 1 and 2 with some modifications and more detailed analysis, and greater verification of calculations with experimental data.

This report indicates that the "effectiveness" of an absorbing slab is proportional to its "reactivity worth," under some simplifying assumptions (which have facilitated the evaluation of the "effectiveness"). These assumptions are as follows:

1. The neutron flux has an isotropic distribution at the surface of the slab.

2. This incident neutron flux has a Maxwellian distribution at thermal energies and a $1/E$ tail at epithermal energies.

3. The slab absorber obeys the single-level, Breit-Wigner law for absorption, with negligible scattering, and allowance is made for overlap of resonance levels.

The above assumptions have facilitated the evaluation of the absorption integral. We deal with single-collision effects, resulting in a general depletion of neutron flux incident at the slab. The justification of these assumptions is as follows:

1. For a heavy absorbing slab, such as encountered in control-rod work, the isotropic P_0 component and the cosine P_1 component (or higher terms in the Legendre expansion of the neutron flux) are nearly equally attenuated by the absorber.

2. In our model of the neutron spectrum, we have neglected small scattering effects by the absorber, and assumed the thermal flux incident on the slab to be a depleted Maxwellian with a kT_n equal to that of the reactor core.

3. Neglect of scattering by the slab is expected to result in small effect, except for materials such as cobalt with Γ_n/Γ_γ near unity at its first resonance level of 132 eV. Ordinarily, this ratio is quite small at low-energy resonance levels of control-rod materials.

II. THE REACTIVITY WORTH OF A CONTROL-ROD SLAB

The reactivity loss due to the insertion of a poison slab in a reactor may be obtained from

$$-\delta\rho = \frac{\int \psi^+ \delta\Sigma_a^P \psi \, d\tau}{\int \psi^+ \chi \nu \Sigma_f \psi \, d\tau} \tag{1}$$

where the adjoints are nonperturbed, the real fluxes are the perturbed values of the fluxes, $\delta\Sigma_a^P$ refers to the poison slab, χ refers to fission spectrum, and $d\tau = dE\, dV$.

In Eq. 1, the ψ's have angular distributions of neutron velocity vectors $\psi(r, v, \mu)$ and satisfy Boltzmann's transport equation.

For a P_1 approximation outside the slab, the directional fluxes incident to the slab surface will be (see Fig. 1)

$$\psi(\mu) = \tfrac{1}{2}\phi + \tfrac{3}{2} j\mu \quad \text{for } 0 < \mu \leq 1, \tag{2}$$

where ϕ is the integrated over angle flux, and j is the net current into the slab from the adjacent media. These two terms of Eq. 2 represent also the isotropic P_0 and cosine-dependent P_1 components of the neutron flux.

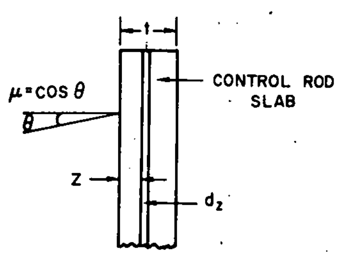

112-8164

Fig. 1. Neutron Flux Incident on Slab

For strongly absorbing slabs, such as encountered in control-rod work, the attenuation of the P_0 and P_1 terms in the slab is nearly the same (see Appendix A). There should, therefore, result only small errors in assuming an isotropic distribution of neutron flux incident to the surface of the slab. Equation 3 may be justified also if we consider that the adjoints ψ^+ of Eq. 1 are nearly space-isotropic, and hence, because of the orthogonality properties of the Legendre's polynomials, we need to consider only the isotropic component of flux, $\phi(\mu)$. Equation 1 may be written, then, in the form

$$-\delta\rho = \frac{\int \phi^+ \delta \Sigma_a^P \phi \, d\tau}{\int \phi^+ \chi \nu \Sigma_f \phi \, d\tau}. \tag{3}$$

Using matrix notation, and three-group theory, we can put Eq. 3 in the form

$$-\delta\rho = \frac{\displaystyle\int_{slab} \left\{ [\phi_1^+ \phi_2^+ \phi_3^+] \begin{bmatrix} \delta\Sigma_{a_1}^P & 0 & 0 \\ 0 & \delta\Sigma_{a_2}^P & 0 \\ 0 & 0 & \delta\Sigma_{a_3}^P \end{bmatrix} \begin{bmatrix} \phi_1 \\ \phi_2 \\ \phi_3 \end{bmatrix} \right\} d\tau}{\displaystyle\int_{core} \left\{ [\phi_1^+ \phi_2^+ \phi_3^+] \begin{bmatrix} 0 & \chi_1 \nu_2 \Sigma_{f_2} & \chi_1 \nu_3 \Sigma_{f_3} \\ 0 & 0 & 0 \\ 0 & 0 & 0 \end{bmatrix} \begin{bmatrix} \phi_1 \\ \phi_2 \\ \phi_3 \end{bmatrix} \right\} d\tau}. \tag{4}$$

We assume for the fast group 1, $\Sigma_{a_1} = 0$, $\chi_2 = \chi_3 = 0$, and $\nu_2 = \nu_3$. Equation 4 becomes, then,

$$-\delta\rho = \frac{\overline{\phi_2^+}(\text{slab}) \displaystyle\int_{slab} \delta\Sigma_{a_2}^P \phi_2 \, d\tau + \overline{\phi_3^+}(\text{slab}) \int_{slab} \delta\Sigma_{a_3}^P \phi_3 \, d\tau}{\overline{\phi_1^+}(\text{core}) \displaystyle\int_{core} \chi_1 (\nu\Sigma_{f_2}\phi_2 + \nu\Sigma_{f_3}\phi_3) \, d\tau}, \tag{5}$$

where $\overline{\phi_2^+}(\text{slab})$ and $\overline{\phi_3^+}(\text{slab})$ are defined as

$$\overline{\phi_i^+}(\text{slab}) = \frac{\displaystyle\int_{slab} \phi_i^+ \delta\Sigma_{ai}^P \phi_i \, d\tau}{\displaystyle\int_{slab} \delta\Sigma_{ai}^P \phi_i \, d\tau}.$$

A. Integration of Numerator in Eq. 5

The integral expressions in the numerator of Eq. 5 may be determined from an evaluation of the absorption integral,

$$A_t = N \int_0^\infty \int_0^t \int_0^1 \mu\phi(E, z, \mu)\ \sigma(E)\ e^{-N\sigma z/\mu}\ d\mu \frac{dz}{\mu}\ dE, \qquad (6)$$

$A_t \equiv$ "effectiveness" of the rod,

where

$$\mu\phi(E, \Omega)\ dE\ d\Omega = \mu\phi(E, \mu)\ dE\ d\mu$$

denotes the number of neutrons contained in an element of solid angle $d\Omega$ with energies between E and $E + dE$, which cross at right angles a unit area of the slab, per second (see Fig. 1). The factor $e^{-N\sigma z/\mu}$ denotes the number of these neutrons that penetrate the purely absorbing slab to a depth z, and the factor $N\sigma dz/\mu$ gives the number of neutrons absorbed in the layer dz.

In Eq. 6, scattering has been neglected, and depletion of incident neutrons allowed for by the use of depletion factors β_i, where i refers to energy group.

The integration of Eq. 6 is carried out for an isotropic spatial distribution of neutrons incident on a face of the slab, where the energy distribution of the neutrons is assumed to be Maxwellian with an appended $1/E$ tail. That is,

$$\left\{\begin{array}{lll} \phi_{\text{thermal}} = \dfrac{E}{(kT_n)^2} e^{-E/kT_n} & & \text{for } 0 \le E \le 0.625 \text{ eV} \\[2ex] \phi_{\text{epi}} = \left(\dfrac{\overline{\Sigma}_a(kT_n)}{\xi\Sigma_s(E_1)}\right)\left(\dfrac{1}{E}\right) & & E > 0.625 \text{ eV} \\[2ex] \quad = C/E & & E_1 = 0.625 \text{ eV} \end{array}\right. \qquad (7)$$

where kT_n refers to the most probable value of effective neutron energy for a Maxwellian distribution of neutron flux.

In Eq. 6, $\sigma_a(E)$ is assumed to obey (as already stated) the single-level Breit-Wigner law,[6]

$$\sigma_\gamma(E) = \pi\lambda\!\!\!^{-2} g \frac{\Gamma_n \Gamma_\gamma}{(E - E_0)^2 + (\Gamma/2)^2} \qquad (8)$$

where

$$\lambda\!\!\!^{-} = \frac{\lambda}{2\pi},$$

$$\lambda = \text{neutron wavelength} = \frac{2.86 \times 10^{-9}}{\sqrt{E}},$$

and g, Γ_n, Γ_γ, and E_0 have their usual meanings.

At resonance energy E_0,

$$\sigma_\gamma(E_0) = \frac{2.6 \times 10^6}{\sqrt{E_0}}\, g\, \frac{\Gamma_n^0 \Gamma_\gamma}{\Gamma^2} \text{ barns}, \tag{9}$$

where

$$\Gamma_n^0 = \Gamma_n/\sqrt{E}.$$

For $E \ll E_0$, and $\Gamma \ll E_0$, Eq. 8 yields

$$\sigma_\gamma(E) = \frac{0.65 \times 10^6}{E_0^2}\, g\, \frac{\Gamma_\gamma \Gamma_n^0}{E^{1/2}}. \tag{10}$$

For $E \gg E_0$, and $\Gamma \ll E_0$, similarly we obtain

$$\sigma_\gamma(E) = 0.65 \times 10^6\, g\, \frac{\Gamma_\gamma \Gamma_{no}}{E^{5/2}}. \tag{11}$$

Since σ_γ varies rapidly with E, we use the modified form of the Breit-Wigner law; i.e.,

$$\sigma_\gamma = \frac{\sigma_0}{1 + x^2},$$

where

$$x = \frac{E - E_0}{\Gamma/2},$$

and

$$\sigma_0 = 4\pi \lambda\!\!\!^{-}{}_0^2 g \frac{\Gamma_n \Gamma_\gamma}{\Gamma^2}\left(\frac{E_0}{E}\right)^{1/2}.$$

The integral of Eq. 6 may be evaluated as the absorption of

a. Maxwellian flux by a $1/V$ absorber.

b. $1/E$ flux by a $1/V^n$ absorber, where $n > 0$.

c. $1/E$ flux by a resonance absorber.

J. Ernest Wilkins, Jr., (in 1946) integrated Eq. 6 and his work is assembled in Ref. 7. A few minor corrections are to be made in the latter report. Also, some of our results are different in form from those given in Ref. 7. Appendix B gives details of our calculations for the absorption of $1/E$ neutron flux by a $1/V^n$ absorber.

The evaluation of the integral of Eq. 6 for absorption of neutrons from both surfaces of the poison slab per unit area of a large slab yields (from Ref. 7 and Appendix B)

$$A_t = \beta_1 F_1(y) + C\left[\frac{\beta_2 F_2(x)}{n} + \beta_3 \frac{\sqrt{\pi}}{2} F_3(X) \cdot \sqrt{Nt} \sum_j \sum_i \frac{\overline{C_j \sigma_{0ij}^{1/2}} \Gamma_{\gamma ij}}{E_{0ij}}\right], \qquad (12)$$

where

β_i's are depletion factors of neutron flux incident on the slab,

$y = Nt\sigma_a(kT_n)$, $x = Nt\sigma_a(E_1)$, and $E_1 = 0.625$ eV,

C_j = the isotopic concentration and j refers to the number of isotopes present,

and

$F_1(y)$ = fraction of thermal neutrons incident on surface of slab, that is absorbed.

<u>For large y</u>

$$F_1(y) = 1 - 2.05\left(\frac{y}{2}\right)^{1/3} \exp\left[-3\left(\frac{y}{2}\right)^{2/3}\right]\left[1 + \frac{5}{36}\left(\frac{y}{2}\right)^{2/3} - \frac{35}{2592}\left(\frac{y}{2}\right)^{4/3}\right] \dots .$$

<u>For small y</u>

$$F_1(y) = \sqrt{\pi}\, y\left[1 + \frac{y}{\sqrt{\pi}}(\ln y)(1 + y^2/12) + 0.1307y - \frac{y^2}{3} - 0.006954y^3\right]$$

Figure 2 is a plot of $F_1(y)$ vs y.

$$\frac{CF_2(x)}{n} = \text{absorption of epithermal } 1/E \text{ flux by a } 1/V^n \text{ absorber } (n > 0) \text{ (see Appendix B).}$$

$$F_2(x) = 1.077 + \ln x + E_1(x) - E_3(x).$$

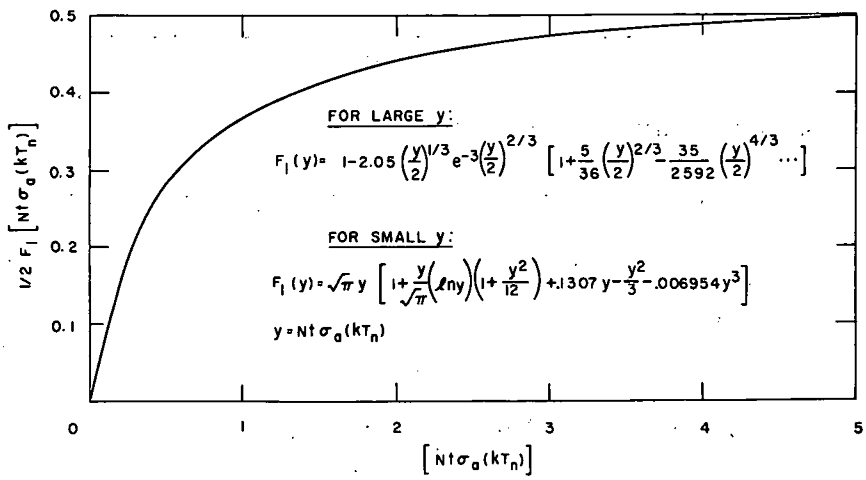

112-8166

Fig. 2. $F_1(y)$ Absorption of Neutrons Having a Maxwellian Distribution by a 1/v Absorber

Figure 3 is a plot of $F_2(x)$ vs x.

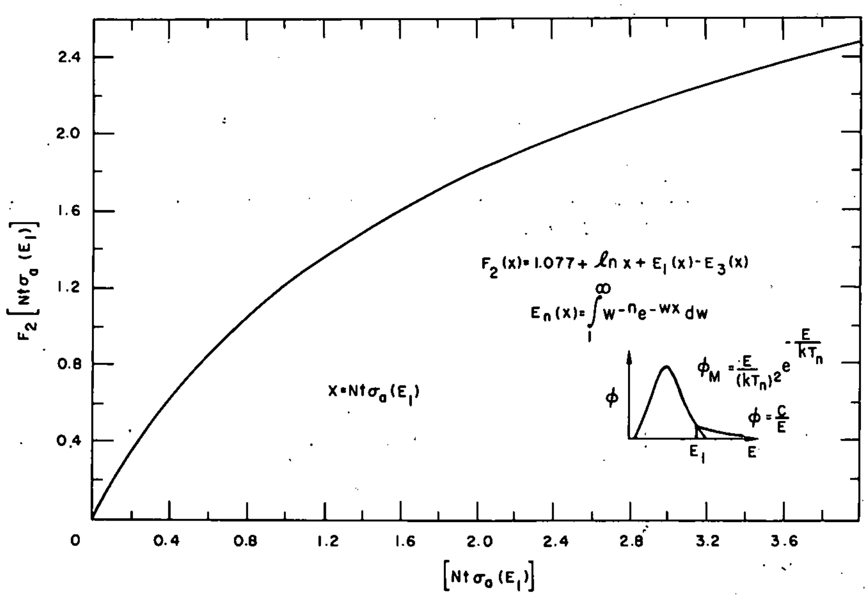

112-8165

Fig. 3. $F_2(x)$ Absorption of Neutrons Having a 1/E Distribution by a 1/v Absorber

$\beta_1(y)$ is a function of y; $\beta_2(x)(< \beta_1)$ is usually of little importance since $\beta_2 F_2(x)$ is ordinarily small. $\beta_3(x)$ depends on strength of resonance. From practical considerations, the above depletion factors may be lumped into one, given by

$$\overline{\beta(y)} \approx \frac{\beta_1 F_1(y) + C\left[\beta_2 F_2(x) + \beta_3\ 1.08\sqrt{Nt}\ \sum_j \sum_i \frac{\overline{C_j \sigma_0^{1/2}}\ \Gamma_{\gamma ij}}{E_{0_{ij}}}\right]}{A_t},$$

where $\overline{\beta(y)}$ may be obtained empirically (see Fig. 4).

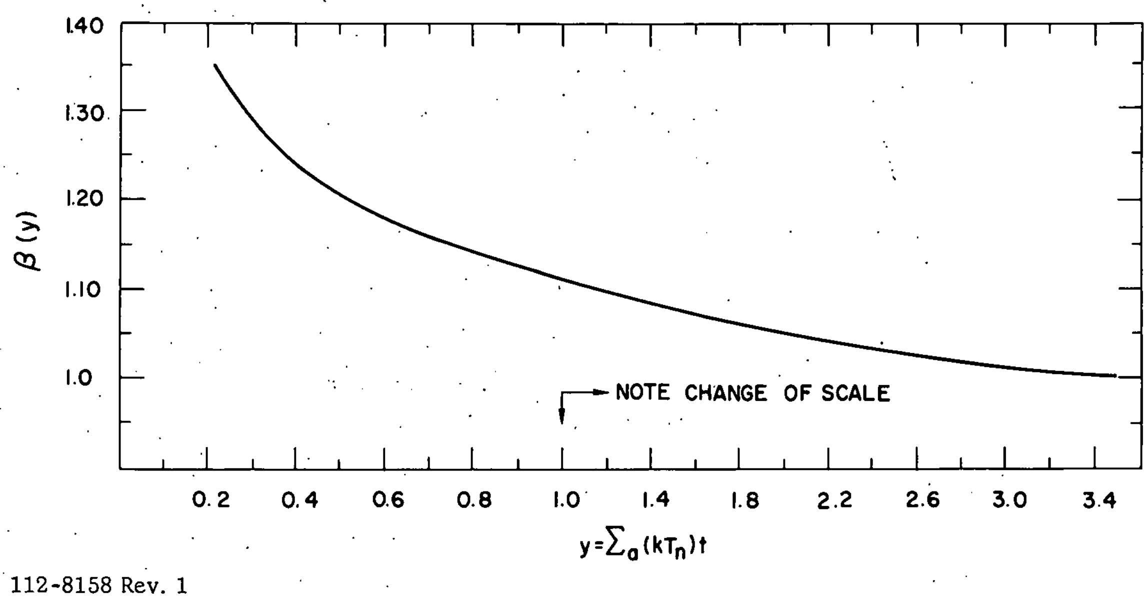

Fig. 4. β(y) Neutron Depletion Factor

$$F_3(X) = \frac{4}{3} - \frac{1}{10X} - \frac{3}{224X^2} \approx \frac{4}{3} \text{ for heavy resonance absorbers,}$$

where

$$X = \frac{1}{2} N\sigma_0 t.$$

The integral expression in the denominator of Eq. 5 may be put in the form

$$\nu\left(\overline{\Sigma}_{f_3} + \frac{\overline{\phi_2}}{\overline{\phi_3}}\ \overline{\Sigma}_{f_2}\right) V_c\, \overline{\phi_3}_{(core)}, \tag{13}$$

where

$$\overline{\Sigma}_{f_i} = \frac{\int_{\text{core}} \phi_i \Sigma_f \, dV}{\int_{\text{core}} \phi_i \, dV},$$

and

$$\overline{\phi}_i = \frac{\int_{\text{core}} \phi \, dV}{\int_{\text{core}} dV}.$$

From Eqs. 6, 12, and 13, it follows that

$$-\delta\rho = \left[\frac{\overline{\phi_3^+}(\text{slab})}{\overline{\phi_1^+}(\text{core})}\right] \frac{\beta\left\{F_1(y) + \frac{\overline{\phi_2^+}}{\overline{\phi_3^+}} C\left[\frac{F_2(x)}{n} + 1.18\sqrt{Nt}\sum_j\sum_i \frac{\overline{C_j \sigma_{0_{ij}}^{1/2}} \Gamma_{\gamma ij}}{E_{0_{ij}}}\right]\right\} S_{\text{eff}}^{\text{slab}} \phi_{3,0}}{\nu\left(\overline{\Sigma}_{f_3} + \frac{\overline{\Phi_2}}{\overline{\Phi_3}}\overline{\Sigma}_{f_2}\right)_{\text{core}} V_c \overline{\Phi_3}(\text{core})}, \quad (14)$$

where

$S_{\text{eff}}^{\text{slab}}$ = effective surface area of slab, allowing for variation of neutron flux in directions parallel to the surface of the slab,

$S_{\text{eff}}^{\text{slab}} \phi_{3,0}$ = total thermal flux incident to the surface of the slab,

and

V_c = volume of core.

For a given reactor with different absorbing slabs of the same dimensions, the quantity

$$\frac{\overline{\phi_3^+}(\text{slab})}{\overline{\phi_1^+}(\text{core})} \frac{S_{\text{eff}}^{\text{slab}} \phi_{3,0}}{\nu\left(\Sigma_{f_3} + \frac{\overline{\Phi_2}}{\overline{\Phi_3}}\Sigma_{f_2}\right) V_c \overline{\Phi_3}(\text{core})} = \frac{1}{Z} \quad (15)$$

is a constant. It follows from Eqs. 14 and 15 that

$$\frac{\bar{\beta}\left\{F_1(y) + \left(\frac{\overline{\phi_2^+}}{\overline{\phi_3^+}}\right)_{(\mathrm{slab})} C\left[\frac{F_2(x)}{n} + 1.18\sqrt{Nt}\sum_j\sum_i \frac{\overline{C_j\sigma_{0_{ij}}^{1/2}\Gamma_{\gamma ij}}}{E_{0_{ij}}}\right]\right\}}{\delta\rho} \tag{16}$$

is also nearly constant.

The ratio $\overline{\phi_2^+}/\overline{\phi_3^+}$ has been evaluated for a number of thermal to intermediate reactors, at or near the axis of the reactor, and was ≈ 0.9 (see Table I). In the present work, this ratio is taken to be 1.0. Equation 16 becomes, then,

$$\frac{\bar{\beta}\left\{F_1(y) + C\left[\frac{F_2(x)}{n} + 1.18\sqrt{Nt}\sum_j\sum_i \frac{\overline{C_j\sigma_{0_{ij}}^{1/2}\Gamma_{\gamma ij}}}{E_{0_{ij}}}\right]\right\}}{\delta\rho} \equiv \frac{\beta A_t}{\delta\rho} \simeq \text{Const. } Z,$$

where

$$A_t = F_1(y) + C\left[\frac{F_2(x)}{n} + 1.18\sqrt{Nt}\sum_j\sum_i \frac{\overline{C_j\sigma_{0_{ij}}^{1/2}\Gamma_{\gamma ij}}}{E_{0_{ij}}}\right], \tag{17}$$

$A_t \equiv$ "effectiveness" of the rod.

TABLE I. $\overline{\phi_{epi}^+}/\overline{\phi_{th}^+}$ in Central Region of Core for Various Critical Assemblies[a]

EBWR Loading with Pu + 1 or 2 Shim Zones	Critical Assemblies[b]		
	FPR-13	FPR-11	FPR-12
0.863	0.915	0.894	0.875

[a]The above values refer to central region of the core and are nonperturbed values.
[b]Adjoint flux data obtained using the MACH code and three-group cross-section data from KAPL-1961.[4]

The value of the constant, Z, is specific to a given reactor and depends on dimensions and location of the slab being tested in the reactor, as defined in Eq. 15.

It follows from the foregoing analysis that the worth of a control slab is proportional to $\overline{\beta}A_t$, or $\overline{\beta}\times$ effectiveness. A_t may be evaluated readily with the aid of curves $F_1(y)$ and $F_2(x)$ (Figs. 2 and 3) and cross-section data (see Table II).

TABLE II. Nuclear Data on Control-rod Materials Studied

Element	Nuclei/cm^3	σ_a(0.025 eV)	$\sum_j \sum_i \frac{\overline{C_{ij}\sigma_{0_{ij}}^{1/2}}\Gamma_{\gamma ij}}{E_{0_{ij}}}$
Hf	0.0439×10^{24}	105	$11.4^{(c)}$
Au	0.0590×10^{24}	98.8	5.7
In	0.0382×10^{24}	196	10.7
Ag	0.0586×10^{24}	63	4.4
Co	0.0909×10^{24}	37	0.1
$Eu^{(a)}$	0.0152×10^{24}	4300	17.8
B_{Nat}	(b)	755	-
Cd	0.0438×10^{24}	2450	-

$^{(a)}N^{Eu}$ obtained for density of Eu_2O_3 of 4.44/gm/cm^3; resonance data exclude resonance lines at 0.327 and 0.461 eV.

$^{(b)}$gm/cm^2 data given in GEAP-3201[3] and KAPL-1961[4] for each slab tested.

$^{(c)}$Overlapping effect of resonance lines only ~3% for slab thickness of 0.05 to 0.25 in.

It now remains to show that experimental data agree well with the above results on the basis of measurements obtained in a number of reactors.

B. Experimental Check of Method of Determining the Reactivity Worth of Control-rod Slabs

The simplicity of the absorption integral method of determining the rod worth makes it of practical value in determining the relative worth of control-rod materials for specific reactors.

Tables III-VII give the measured reactivity worth, $\delta\rho^{adj}_{meas}$, and calculated βA_t values and their ratio, $Z = \beta A_t/\delta\rho^{adj}_{meas}$, for a large number of slabs tested in water-moderated ZPR-1 and critical assembly described in GEAP-3201,[3] and in three polyethylene-moderated critical assemblies described in KAPL-1961.[4] The latter assemblies, FPR-13, FPR-11, and FPR-12, have values of

$$C = \frac{\Sigma_a(kT_n)}{\xi\Sigma_s(\infty)}$$

of 0.08, 0.396 and 0.71, respectively. FPR-11 and FPR-12 have loadings of intermediate reactors (with N^H/N^{25} values of 54.6 and 30, respectively) and should offer more of an acid test to the method used.

TABLE III. Ratios of Calculated Effectiveness over Measured Reactivity Worths of Various Poison Slabs, Measured in ZPR-1

Slab Thickness, in.	Worth, dollars	$\delta\rho_{meas}$, dollars x β_{eff} [(a)]	$\delta\rho_{meas}^{adj}$ [(b)]	y	A_t	β [(c)]	βA_t	$Z = \frac{\beta A_t}{\delta\rho_{meas}^{adj}}$
Hf								
0.05 Hf	1.55	0.011625	0.011857	0.471	0.6676	1.21	0.8078	68.1
0.10 Hf + 0.095 SS	1.98	0.01485	0.01485	0.941	0.8906	1.125	1.0019	67.5
0.15 Hf	2.19	0.01642	0.01609	1.412	1.0150	1.08	1.0962	68.1
0.15 Hf + 0.095 SS	2.22	0.01665	0.01632	1.412	1.0126	1.08	1.0936	67.0
0.20 Hf	2.38	0.01785	0.01714	1.888	1.110	1.05	1.165	68.0
0.25 Hf	2.47	0.01852	0.01759	2.353	1.1788	1.03	1.2141	69.0
Au								
0.05	1.57	0.01177	0.0120	0.5925	0.6862	1.174	0.8056	67.1
0.10	2.00	0.0150	0.0150	1.185	0.8886	1.098	0.9756	65.0
0.15	2.13	0.01597	0.01565	1.7776	1.0061	1.055	1.0614	67.7
0.20	2.34	0.01755	0.01685	2.370	1.0853	1.030	1.1178	66.3
0.25	2.40	0.01800	0.0171	2.9627	1.1360	1.016	1.1541	67.4
Cd-Ag								
0.10	2.04	0.0153	0.0153	>10	1.0748	1.0	1.0748	70.2
0.19	2.29	0.01717	0.01648	>10	1.1054	1.0	1.1054	67.0
0.25	2.37	0.01777	0.01688	>10	1.1255	1.0	1.1255	66.6
0.29	2.48	0.018637	0.01752	>10	1.1368	1.0	1.1368	64.8
0.10 Hf + 0.02 Cd + 0.10 Hf	2.52	0.01890	0.01814	>5	1.2284	1.0	1.2284	67.7
0.10 Hf + 0.02 Al + 0.10 (Cd-Ag)	2.50	0.01875	0.01800	>10	1.2325	1.0	1.2325	68.4
Co								
0.075	1.25	0.009375	0.00946	0.5124	0.5762	1.19	0.6856	72.3
0.125	1.51	0.011325	0.01121	0.8540	0.7192	1.135	0.8163	72.7
0.175	1.69	0.012675	0.01229	1.1957	0.7994	1.097	0.8769	71.3
0.225	1.84	0.013800	0.01327	1.5373	0.8622	1.07	0.9225	69.4
							Average $\overline{Z}$ =	68.1
							Average Deviation = $\overline{\Delta Z}$ =	1.5 (2.2%)

[(a)] β_{eff} = 0.0075.

[(b)] $\delta\rho_{meas}^{adj} = \delta\rho_{meas}$ x edge correction factor.

[(c)] β refers to neutron-flux nondepletion factor at surface of poison slab.

TABLE IV. Ratios of Calculated Effectiveness over Measured Reactivity Worths, Reported in GEAP-3201 for Various Poison Slabs

Slab	Thickness, in.	Surface Density, gm/cm^2	$(RW)_{corr}$ [(a)]	$y = \sum_a (kT_n)t$	β [(b)]	A_t	βA_t	$Z = \frac{\beta A_t}{(RW)_{corr}}$
Hf	0.025	0.856	0.572	0.234	1.42	0.437	0.6205	1.084
	0.045	1.476	0.726	0.421	1.24	0.625	0.7744	1.067
	0.103	3.422	0.920	0.9642	1.115	0.883	0.9845	1.070
	0.206	6.833	1.051	1.9275	1.050	1.102	1.157	1.100
	0.276	9.175	1.106	2.582	1.025	1.191	1.220	1.103
Au	0.027	1.318	0.504	0.319	1.325	0.464	0.6178	1.095
	0.051	2.518	0.719	0.609	1.17	0.677	0.792	1.100
	0.101	4.926	0.868	1.192	1.10	0.871	0.959	1.103
	0.196	9.606	0.987	2.32	1.033	1.038	1.073	1.088
	0.297	14.531	1.038	3.52	1.00	1.142	1.142	1.101
B (B-glass)	0.152	0.0335	0.7503	0.9706	1.115	0.778	0.8675	1.156
	0.101	0.0478	0.8144	1.3847	1.082	0.866	0.938	1.152
	0.302	0.0664	0.8756	1.924	1.048	0.952	0.997	1.140
	0.200	0.0880	0.9282	2.5495	1.025	1.018	1.044	1.126
	0.275	0.1206	0.9728	3.494	1.00	1.079	1.079	1.110
	0.104	0.1575	1.0062	4.563	1.00	1.131	1.131	1.026
	0.206	0.3026	1.0867	8.767	1.00	1.201	1.201	1.106
	0.290	0.4241	1.1326	12.287	1.00	1.235	1.235	1.090

TABLE IV (Contd.)

Slab	Thickness, in.	Surface Density, gm/cm^2	$(RW)_{corr}$[a]	$y = \sum_a (kT_n)t$	β[b]	A_t	βA_t	$Z = \frac{\beta A_t}{(RW)_{corr}}$
In	0.025	0.468	0.632	0.3783	1.27	0.560	0.711	1.125
	0.050	0.928	0.785	0.7567	1.150	0.7646	0.880	1.121
	0.100	1.858	0.908	1.5137	1.072	0.9674	1.038	1.142
	0.201	3.697	0.998	3.042	1.015	1.1450	1.162	1.166
	0.301	5.554	1.036	4.556	1.00	1.2354	1.235	1.192
Ag	0.027	0.717	0.455	0.2007	1.50	0.342	0.5130	1.127
	0.052	1.376	0.617	0.3851	1.270	0.5592	0.710	1.151
	0.103	2.746	0.798	0.7686	1.146	0.768	0.880	1.102
	0.196	5.226	0.944	1.4628	1.075	0.963	1.035	1.098
	0.299	7.970	1.021	2.2308	1.035	1.090	1.129	1.103
Co	0.098	2.187	0.663	0.66	1.16	0.672	0.780	1.176
	0.154	3.418	0.759	1.068	1.11	0.795	0.883	1.162
	0.252	5.601	0.855	1.745	1.056	0.919	0.970	1.135
Eu_2O_3	0.05	0.561	1.032	2.979	1.015	1.087	1.188	1.151
	0.174	1.972	1.197	10.47	1.00	1.224	1.3728	1.147
	0.299	3.375	1.253	17.92	1.00	1.278	1.480	1.181
Cd	0.001	0.022	0.494	0.295	1.36	0.42	0.571	1.148
	0.002	0.050	0.648	0.670	1.163	0.642	0.746	1.151
	0.005	0.101	0.728	1.352	1.085	0.804	0.872	1.198
	0.010	0.226	0.789	3.021	1.012	0.948	0.958	1.213
							Average Z =	1.126
							Average Deviation = $\overline{\Delta Z}$ =	0.032 (2.8%)

(a)Relative worth RW = $(\rho_0 - \rho_x)/(\rho_0 - \rho_{std})$, with edge correction.
(b)β refers to neutron-flux nondepletion factor at surface of poison slab.

TABLE V. Ratios of Calculated Effectiveness over Measured Reactivity Worths of Various Poison Slabs,[a] Measured in FPR-13.

Slab	Thickness, in.	Worth, dollars	$\delta\rho_{meas}$, dollars x β_{eff}[b]	$\delta\rho_{meas}^{adj}$ (c)	$y = \sum_a (kT_n)t$	β[d]	A_t	βA_t	$Z = \frac{\beta A_t}{\delta\rho_{meas}^{adj}}$
Hf	0.05	2.227	0.01703	0.01720	0.4935	1.20	0.6534	0.7841	45.6
	0.10	2.677	0.020479	0.020479	0.987	1.12	0.8648	0.9685	47.3
	0.15	2.968	0.022705	0.022470	1.480	1.075	0.9736	1.0467	46.6
	0.20	3.164	0.024204	0.023700	1.974	1.045	1.0760	1.124	47.4
	0.25	3.267	0.024992	0.02425	2.468	1.027	1.1382	1.1689	48.2
In	0.05	2.358	0.01804	0.01822	0.796	1.142	0.7584	0.8661	47.5
	0.10	2.781	0.02127	0.02127	1.592	1.067	0.9482	1.0117	47.5
	0.15	2.976	0.02276	0.02254	2.388	1.030	1.0534	1.0850	48.1
	0.20	3.117	0.0240	0.0235	3.184	1.008	1.1080	1.1168	47.5
B^{Nat}[e]	0.10	2.442	0.01868	0.01868	1.2754	1.09	0.824	0.8981	48.0
Ag	0.05	1.881	0.01439	0.01453	0.3927	1.25	0.5461	0.6826	46.9
	0.10	2.423	0.018536	0.01853	0.7854	1.145	0.7435	0.8513	45.9
	0.15	2.711	0.02074	0.02053	1.1781	1.10	0.8596	0.9447	46.0
	0.20	2.922	0.02235	0.02191	1.5708	1.068	0.9374	1.0011	45.7
	0.25	3.066	0.02345	0.02283	1.9635	1.045	1.0002	1.0452	45.8
13.85 w/o Eu_2O_3 in SS	0.10	2.789	0.02133	0.02133	3.2	1.00	1.039	1.039	48.7
								Average Z =	47.0
								Average Deviation = $\overline{\Delta Z}$ =	0.8 (1.8%)

(a)Measurements data taken from KAPL-1961,[4] for FPR-13 Critical Assembly.

(b)β_{eff} = 0.00765.

(c)$\delta\rho_{meas}^{adj}$ = $\delta\rho_{meas}$ x edge correction factor.

(d)β refers to neutron-flux nondepletion factor at surface of poison slab.

(e)0.0368 gm/cm^2 of B^{Nat} in Al.

TABLE VI. Ratios of Calculated Effectiveness over Measured Reactivity Worths of Various Poison Slabs,[a] Measured in FPR-11.

Slab	Thickness, in.	Worth, dollars	$\delta\rho_{meas}$ dollars x β_{eff}[b]	$\delta\rho^{adj}_{meas}$,[c]	$y = \sum_a (kT_n)t$	β[d]	A_t	$\bar{\beta}A_t$	$Z = \frac{\beta A_t}{\delta\rho^{adj}_{meas}}$
Hf	0.05	1.040	0.008080	0.008161	0.4474	1.22	0.9648	1.177	144.2
	0.10	1.378	0.01071	0.01071	0.8948	1.13	1.3696	1.5476	144.5
	0.15	1.576	0.01224	0.01212	1.342	1.085	1.623	1.761	145.2
	0.20	1.700	0.01320	0.0130	1.789	1.055	1.8405	1.9417	149.3
	0.25	1.815	0.01410	0.01373	2.3370	1.03	2.0227	2.085	152
In	0.05	1.005	0.00781	0.00789	0.725	1.15	1.034	1.191	151
	0.10	1.276	0.00991	0.00991	1.45	1.075	1.362	1.464	147.6
	0.15	1.426	0.01108	0.01097	2.175	1.04	1.571	1.631	148.6
	0.20	1.535	0.01193	0.01157	2.90	1.015	1.719	1.745	150.8
B^{Nat}	0.10	0.950	0.00738	0.00738	1.306	1.09	0.990	1.0791	146.2
Ag	0.05	0.752	0.00584	0.00591	0.3583	1.25	0.7115	0.889	150
	0.10	1.065	0.00827	0.00827	0.716	1.155	1.0325	1.1925	144
	0.15	1.269	0.00986	0.00976	1.075	1.11	1.2408	1.3773	141
	0.20	1.433	0.01113	0.01091	1.433	1.083	1.394	1.5083	138
	0.25	1.557	0.01210	0.01178	1.7915	1.055	1.5334	1.6177	137
13.85 w/o Eu_2O_3 in SS	0.10	1.254	0.009743	0.009743	3.2	1.0	1.391	1.391	145.2
								Average Z =	146
								Average Deviation = $\overline{\Delta Z}$ =	3.5 (2.4%)

(a)Measurements data taken from KAPL-1961,[4] for FPR-11 Critical Assembly.

(b)β_{eff} = 0.00777.

(c)$\delta\rho^{adj}_{meas} = \delta\rho_{meas}$ x edge correction factor.

(d)β refers to neutron-flux nondepletion factor at surface of poison slab.

(e)0.0368 gm/cm^2 of B^{Nat} in Al.

TABLE VII. Ratios of Calculated Effectiveness over Measured Reactivity Worths of Various Poison Slabs,[a] Measured in FPR-12.

Slab	Thickness, in.	Worth, dollars	$\delta\rho_{meas}$ dollars x β_{eff}[b]	$\delta\rho^{adj}_{meas}$,[c]	$y = \sum_a (kT_n)t$	β[d]	A_t	$\bar{\beta}A_t$	$Z = \frac{\beta A_t}{\delta\rho^{adj}_{meas}}$
Hf	0.05	0.812	0.00650	0.00650	0.4417	1.215	1.306	1.587	242
	0.10	1.097	0.00878	0.00875	0.8834	1.13	1.890	2.136	243
	0.15	1.273	0.010184	0.01013	1.3251	1.085	2.272	2.472	244
	0.20	1.404	0.011232	0.0113	1.7668	1.660	2.614	2.770	252
	0.25	1.504	0.012032	0.0123	2.208	1.040	2.895	3.010	256
In	0.05	0.745	0.00596	0.00635	0.712	1.155	1.3422	1.550	257
	0.10	0.958	0.007664	0.00790	1.424	1.078	1.789	1.93	252
	0.15	1.085	0.00868	0.00916	2.136	1.04	2.147	2.235	260
	0.20	1.167	0.00934	0.00975	2.848	1.017	2.3390	2.38	259
B^{Nat}	0.10	0.668	0.00534	0.005053	1.1408	1.102	1.119	1.233	231
Ag	0.05	0.553	0.00442	0.00461	0.3528	1.25	0.9006	1.125	251
	0.10	0.807	0.00645	0.00638	0.7056	1.155	1.3323	1.5388	239
	0.15	0.986	0.00788	0.007406	1.0583	1.11	1.628	1.8070	231
	0.20	1.122	0.00897	0.008226	1.4112	1.08	1.8552	2.0072	228
	0.25	1.232	0.00985	0.008972	1.7640	1.055	2.0614	2.1892	228
13.85 w/o Eu_2O_3 in SS	0.10	0.958	0.007664	0.007342	3.2	1.0	1.7916	1.7916	234
								Average Z =	243
								Average Deviation = $\overline{\Delta Z}$ =	9.3 (3.8%)

(a)Measurements data taken from KAPL-1961,[4] for FPR-12 Critical Assembly.

(b)β_{eff} = 0.0080.

(c)$\delta\rho^{adj}_{meas} = \delta\rho_{meas}$ x edge correction factor.

(d)β refers to neutron-flux nondepletion factor at surface of poison slab.

(e)0.0368 gm/cm^2 of B^{Nat} in Al.

Our calculations of A_t do not allow for absorption by the edges of the slabs. Accordingly, measured reactivity data have been adjusted by the absorption-area technique.

To detect any possible errors in measured or calculated data, plots of $\delta\rho_{meas}$ and $\delta\rho_{calc}$ vs slab thickness were obtained. Values of $\delta\rho_{calc}$ were obtained (normalized) by making use of $\overline{Z}$ values; i.e., $\delta\rho_{calc} = \beta A_t/\overline{Z}$, where cross-section data used were obtained from BNL-325,[6]

$$\overline{Z} = \frac{\sum_{i=1}^{n} Z_i}{\text{number of slabs} = n}.$$

C. ZPR-1 Data

These measurements have been reported previously.[1,2]

The average Z of 20 measurements on six slab materials was $\overline{Z}$ = 68.1 with an average deviation of $\overline{\Delta Z}$ = 1.5 (2.2%), and ΔZ_{max} = 6.3% (see Table III). Greater than average discrepancies occurred for cobalt slabs. This may have been due to anomalous scattering by cobalt; its first resonance at 132 eV has a Γ_n/Γ = 0.92. Resonance absorption in cobalt is not only small, but its scattering may actually result in reducing the worth of the rod. Figure 5 shows the $\delta\rho$-vs-thickness characteristics of measured and calculated data.

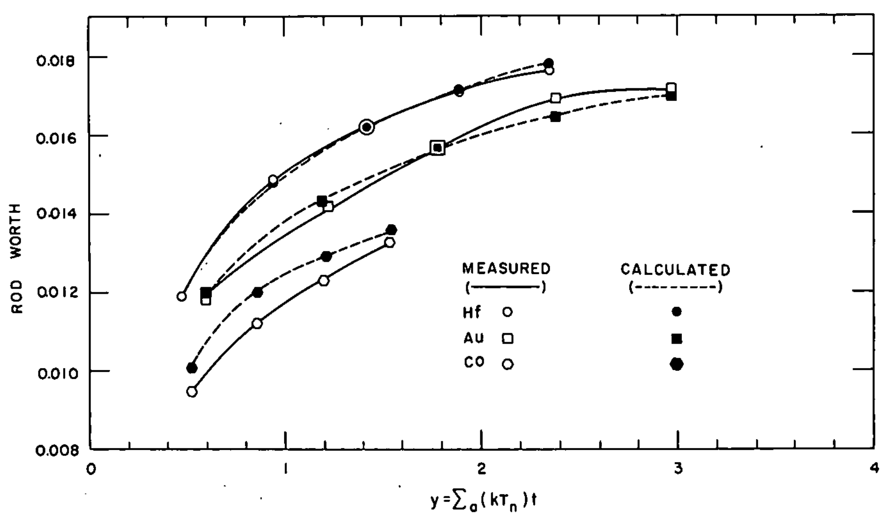

112-8156

Fig. 5. $\delta\rho_{calc}$ and $\delta\rho_{meas}$ vs Slab Thickness in ZPR-1

D. GEAP-3201 Data

The measurements data were obtained from GEAP-3201. These are relative values referred to 0.20-in. cadmium measurements, and there is no need to correct them to absolute worth values, although this could be done readily if required.

The average Z of 38 slabs for eight different slab materials was (see Table IV)

$$\overline{Z} = 1.126,$$

and

$$\overline{\Delta Z} = 0.032\ (2.8\%),$$

with

$$\Delta Z_{max} = 8.7\%\ \text{for}\ Eu_2O_3.$$

Figure 6 shows the $\delta\rho$-vs-thickness characteristics of calculated and measured data for Hf, In, Au, Ag, and B.

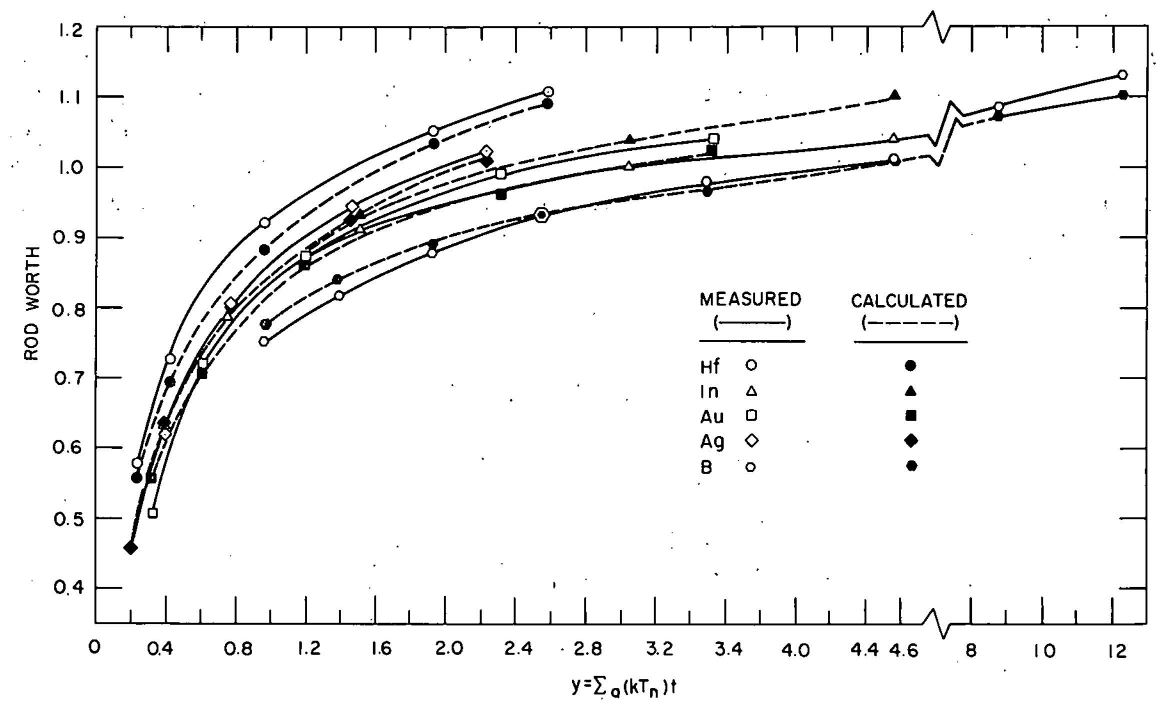

112-8157

Fig. 6. $\delta\rho_{calc}$ and $\delta\rho_{meas}$ vs Slab Thickness in GEAP-3201 Critical Assembly

E. FPR-13 Data

FPR-13 is a thermal reactor, hydrogen-moderated, with a neutron spectrum similar to the previous two reactors. The average Z of 16 measurements on six slab materials was (see Table V)

$$\overline{Z} = 47.0$$

and

$$\overline{\Delta Z} = 0.8\ (1.8\%)$$

with

$$\Delta Z_{max} = 1.6\ (3.4\%).$$

Figure 7 shows the $\delta\rho$-vs-thickness characteristics of calculated and measured data for Hf, In, and Ag.

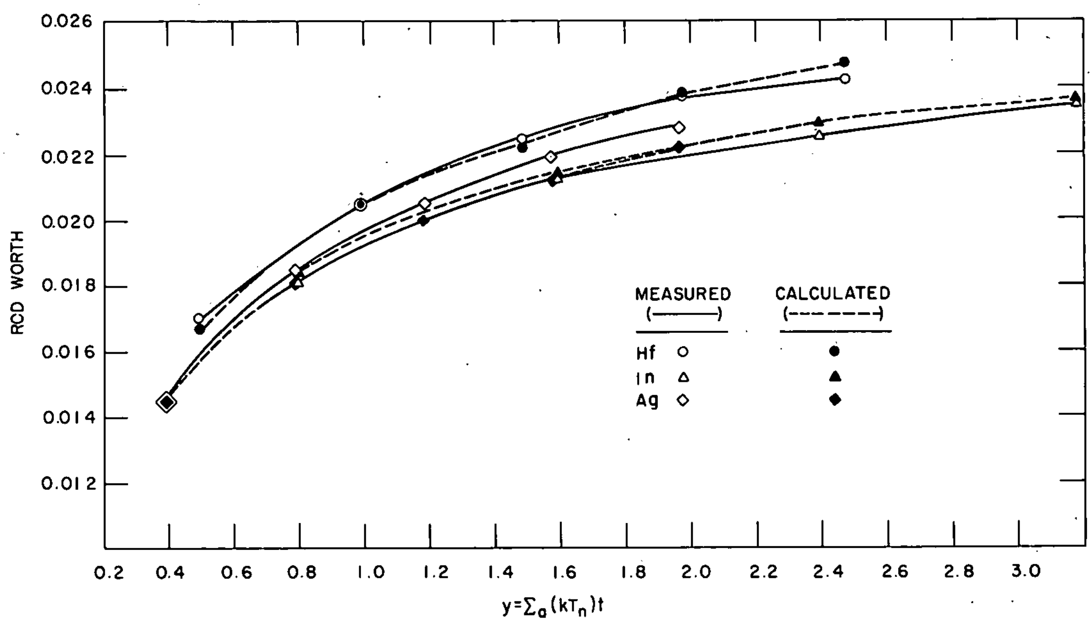

112-8154

Fig. 7. $\delta\rho_{calc}$ and $\delta\rho_{meas}$ vs Slab Thickness in FPR-13

F. FPR-11 and FPR-12 Data

These critical assemblies are in the intermediate range with N^H/N^{25} ratios of ~55 and 30, respectively. The absorption of epithermal neutrons may exceed those of thermals in the FPR-11 and FPR-12 by factors of 1.2 and 2, respectively.

With such heavy absorption of epithermal neutrons, our results should offer a good test of the simple method used.

The average $\overline{Z}$, $\overline{\Delta Z}$, and $\overline{\Delta Z}_{max}$ of these critical assemblies are as follows (see also Tables VI and VII):

	FPR-11	FPR-12
$\overline{Z}$	146	243
$\overline{\Delta Z}$	3.5 (2.4%)	9.3 (3.8%)
$\overline{\Delta Z}_{max}$	8.2 (5.6%)	16 (6.5%)

Figures 8 and 9 show the measured and calculated slab worth-vs-thickness characteristics in FPR-11 and FPR-12.

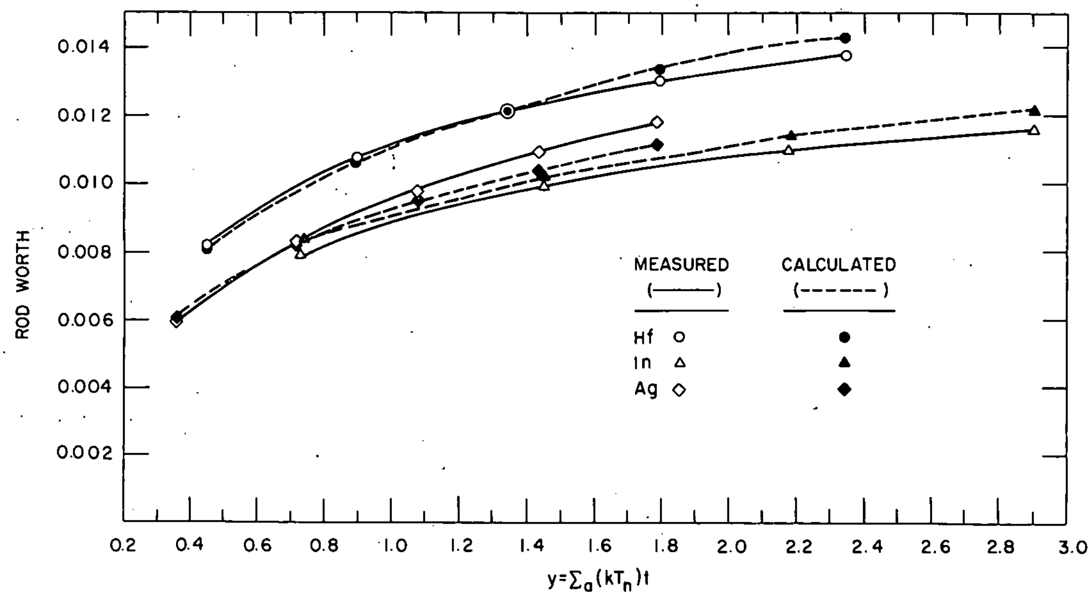

112-8155

Fig. 8. $\delta\rho_{calc}$ and $\delta\rho_{meas}$ vs Slab Thickness in FPR-11

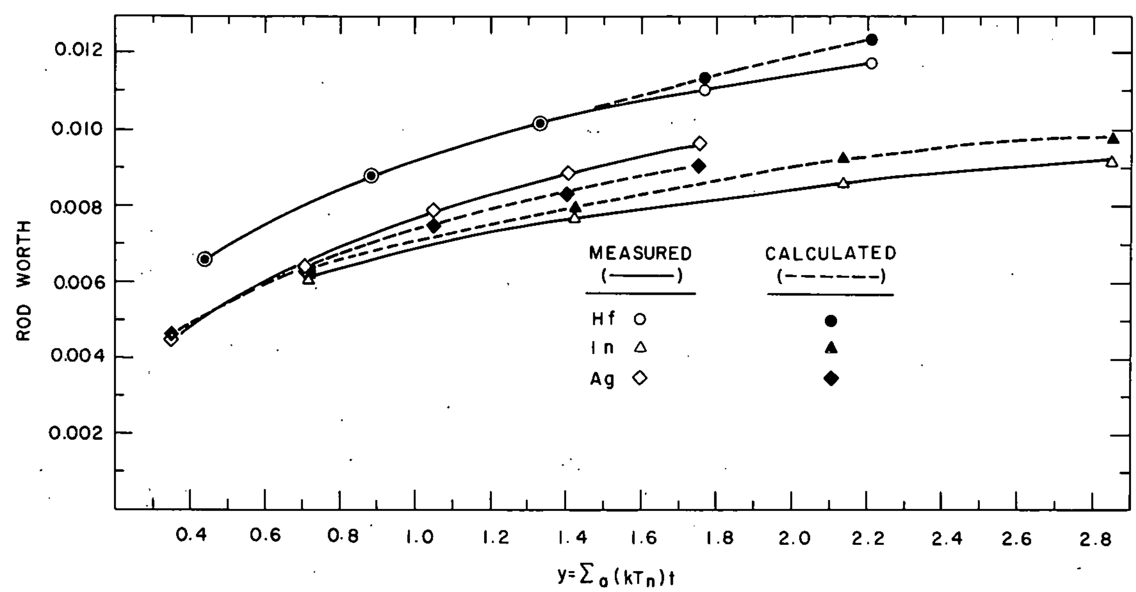

112-8153

Fig. 9. $\delta\rho_{calc}$ and $\delta\rho_{meas}$ vs Slab Thickness in FPR-12

G. Conclusions

We have shown that the reactivity worth of a control-rod slab in a reactor is proportional to the "effectiveness," A_t, multiplied by $\beta(y)$ under some simplifying assumptions. The factor $\beta(y)$ accounts for depletion of incident neutrons.

The effectiveness of a heavy absorber is defined as the absorption integral, A_t, of the poison slabs.

The constancy of the ratio, $\beta A_t/\delta\rho$, has been verified for a variety of slab materials tested in three thermal and two intermediate-range reactors.

To determine the relative effectiveness of a simple (or composite) slab material in a given reactor, we need to evaluate the following parameters (see Table II):

$y = Nt\sigma_a(kT_n) \cdot t$, then obtain $F_1(y)$ from Fig. 2;

$x = Nt\sigma_a(E_1)$ (where $E_1 = 0.625$ eV), then obtain $F_2(x)$

from Fig. 3. We also obtain

$$\sqrt{Nt} \sum_j \sum_i \frac{\overline{C_j \sigma_{0_{ij}}^{1/2}} \Gamma_{\gamma ij}}{E_{0_{ij}}},$$

where i refers to different resonance lines of an isotope, and j refers to different isotopes of the rod material.

We evaluate also the constant,

$$C \approx \frac{\Sigma_a(kT_n)}{\overline{\xi\Sigma_S}(E_1)},$$

where $E_1 \approx 0.625$ eV. We compute now A_t the "effectiveness" with the aid of Eq. 12 and curves of Figs. 2 and 3. The reactivity worth of the rod is proportional to $\overline{\beta}(y)\, A_t$, where $\overline{\beta}(y)$ is obtained from Fig. 4.

APPENDIX A

Proof That Isotropic and Cosine Distributions of Incident Flux Are Attenuated Nearly Equally by a Heavy Absorber

The fraction of neutrons absorbed by a slab with $\Sigma_a t = y$, for an isotropic distribution of incident neutrons, neglecting scattering by the slab, is given by

$$F_0(y) = 1 - 2 \int_0^1 \mu e^{-y/\mu} \, d\mu = 1 - 2E_3(y).$$

The capture fraction for a cosine distribution of incident flux is given (neglecting scattering by the slab, again) by

$$F_1(y) = 1 - 3 \int_0^1 \mu^2 e^{-y/\mu} \, d\mu = 1 - 3E_4(y).$$

Values of $F_0(y)$ and $F_1(y)$ as functions of y are as follows:

$y = \Sigma_a t$	0.5	1.0	1.5	2.0	2.5	3.0	3.5
$F_0(y) = 1 - 2E_3(y)$	0.557	0.7816	0.8865	0.9397	0.9674	0.9821	0.9901
$F_1(y) = 1 - 3E_4(y)$	0.5044	0.7418	0.8620	0.9250	0.9587	0.9770	0.9811
$\frac{F_0(y)}{F_1(y)}$	1.104	1.0536	1.0284	1.0158	1.0090	1.0052	1.0030

It follows from the above that for a heavy absorber, the capture fraction of the isotropic component of neutrons is nearly the same (within a few percent) as that for the cosine distribution of neutrons.

APPENDIX B

Absorption of 1/E Neutron Flux by a $1/v^n$ Absorber $(n > 0)$

The absorption integral becomes

$$A_{epi} = CNc_o \int_0^1 \int_0^t \int_{v_1}^{\infty} v^{-n-1} e^{-Nc_o z/\mu v^n} \, dv \, dz \, d\mu, \qquad (18)$$

where $c_o = \sigma_0 v_0$, and v_0 and v_1 are the neutron speed at 0.0253 eV and the top of thermal group, respectively. If we set $Nc_o z/\mu = \alpha$ and $v^{-n} = \omega$, Eq. 18 becomes

$$A_{epi} = CNc_o \int_0^1 d\mu \int_0^t dz \int_{v_1^{-n}}^{0} e^{-\alpha\omega} \frac{d\omega}{-n}.$$

Integrating over ω, the above integral becomes

$$A_{epi} = CNc_o \int_0^1 \int_0^t \frac{1}{\alpha n}\left(1 - e^{-\alpha v_1^{-n}}\right) dz \, d\mu.$$

Setting $\beta = Nc_o v_1^{-n}$, we obtain $\alpha v_1^{-n} = \beta(z/\mu)$ and $CNc_o/\alpha n = (C/n)(\mu/z)$. Now Aepi becomes

$$A_{epi} = \frac{C}{n} \int_0^1 d\mu \int_0^t \frac{\mu}{z}\left(1 - e^{-\beta(z/\mu)}\right) dz. \qquad (19)$$

Introduce now ζ as variable, $\zeta = \beta(z/\mu)$. Equation 19 becomes

$$A_{epi} = \frac{C}{n} \int_0^1 d\mu \int_0^{x/\mu} \mu\zeta^{-1}(1 - e^{-\zeta}) \, d\zeta, \qquad (20)$$

where $x = \beta t$.

To evaluate Eq. 20, the order of integration is changed. The field of integration consists of two parts, as shown below in shaded areas.

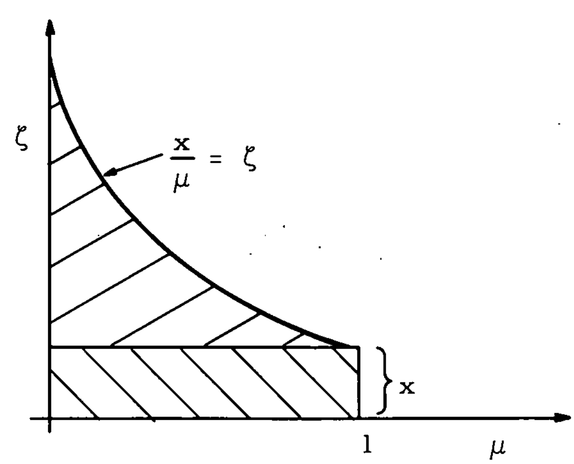

We have

$$A_{epi} = \frac{C}{n}\int_0^1 d\mu \int_0^{x/\mu} \mu\zeta^{-1}(1 - e^{-\zeta})\, d\zeta$$

$$= \frac{C}{n}\int_0^x d\zeta \int_0^1 \mu\zeta^{-1}(1 - e^{-\zeta})\, d\mu + \int_x^\infty d\zeta \int_0^{x/\zeta} \mu\zeta^{-1}(1 - e^{-\zeta})\, d\mu$$

$$= \frac{C}{2n}\left\{\int_0^x \zeta^{-1}(1 - e^{-\zeta})\, d\zeta + x^2 \int_x^{-\infty} \zeta^{-3}(1 - e^{-\zeta})\, d\zeta\right\}. \qquad (21)$$

From MT-1,[9] we have

$$E_n(x) = \int_1^\infty \zeta^{-n}e^{-\zeta x}\, d\zeta = x^{n-1}\int_x^\infty \zeta^{-n}e^{-\zeta}\, d\zeta, \qquad (22)$$

and

$$\int_0^1 \zeta^{-1}(1 - e^{-\zeta})\, d\zeta = E_1(1) + \gamma, \qquad (23)$$

where γ = Euler's constant = 0.5772.

From Eqs. 22 and 23, the first integral in Eq. 21 becomes

$$\int_0^x \zeta^{-1}(1 - e^{-\zeta})\, d\zeta = \int_0^1 \{\quad\} + \int_1^\infty \{\quad\} - \int_x^\infty \{\quad\}$$

$$= [E_1(1)+\gamma] + \left[\ln \zeta\Big|_1^\infty - E_1(1)\right] - \left[\ln \zeta\Big|_x^\infty - E_1(x)\right]$$

$$= \gamma + \ln x + E_1(x). \qquad (24)$$

Similarly, the second integral of Eq. 21 yields

$$\int_x^\infty \zeta^{-3}(1 - e^{-\zeta})\, d\zeta = \frac{1}{2x^2} - x^{-2}E_3(x). \qquad (25)$$

From Eqs. 21, 24, and 25,

$$A_{epi} = \frac{C}{n}\left\{\gamma + \ln x + E_1(x) + \frac{1}{2} - E_3(x)\right\},$$

or

$$A_{epi} = CF_2(x)/n, \qquad (26)$$

where

$$F_2(x) = 1.0772 + \ln x + E_1(x) = E_3(x). \qquad (27)$$

The absorption of $1/E$ neutron flux by a $1/v^n$ absorber (where $n > 0$) is $(1/n)^{th}$ of that for a $1/v$ absorber.

ACKNOWLEDGMENT

The writer wishes to acknowledge the cooperation of Dr. S. Krasner for work done in the initial stages of evaluation work at Argonne National Laboratory (Oct 1951).

REFERENCES

1. H. P. Iskenderian, *Theory and Experiments on Rods Containing Rare Earth Metals*, TID-7532 (Pt. 1), Reactor Control Meeting, Los Angeles, Calif. (1957).

2. H. P. Iskenderian, *Effectiveness of Control Rod Materials*, Nucleonics, Nov 1957, pp. 150-154.

3. R. A. Becker and J. L. Russell, Jr., *Relative Effectiveness of Reactor Control Materials*, GEAP-3201 (1959).

4. D. R. Bach and M. E. Way, *The Worth of Single Control Rods in Hydrogenous Reactors*, KAPL-1961 (1958).

5. A. F. Henry, *A Theoretical Method for Determining the Worth of Control Rods*, WAPD-218 (1959).

6. D. J. Hughes and J. A. Harvey, *Neutron Cross Sections*, BNL-325 (July 1955).

7. J. E. Wilkins, Jr., *The Activations of Thick Foils*, CP-3581 (1946).

8. R. P. Gillespie, *Integration*, p. 37, Oliver and Boyd Interscience Publishers, Inc., New York (1947).

9. G. Placzek, *The Functions* $E_n(x) = \int_1^\infty e^{-xu} u^{-n} dx$, MT-1, National Research Council of Canada, Division of Atomic Energy, Chalk River, Ontario.